JIPB Journal of Integrative Plant Biology

OS1 functions in the allocation of nutrients between the endosperm and embryo in maize seeds[FA]

Weibin Song[†*], Jinjie Zhu[†], Haiming Zhao, Yingnan Li, Jiangtao Liu, Xiangbo Zhang, Liangliang Huang and Jinsheng Lai

State Key Laboratory of Agrobiotechnology and National Maize Improvement Center, Department of Plant Genetics and Breeding, China Agricultural University, Beijing 100094, China
[†]These authors contributed equally to this work.
*Correspondence: Weibin Song (songwb@cau.edu.cn)
doi: 10.1111/jipb.12755

Research Article

Abstract Uncovering the genetic basis of seed development will provide useful tools for improving both crop yield and nutritional value. However, the genetic regulatory networks of maize (*Zea mays*) seed development remain largely unknown. The maize *opaque endosperm and small germ 1* (*os1*) mutant has opaque endosperm and a small embryo. Here, we cloned *OS1* and show that it encodes a putative transcription factor containing an RWP-RK domain. Transcriptional analysis indicated that *OS1* expression is elevated in early endosperm development, especially in the basal endosperm transfer layer (BETL), conducting zone (CZ), and central starch endosperm (CSE) cells. RNA sequencing (RNA-Seq) analysis of the *os1* mutant revealed sharp downregulation of certain genes in specific cell types, including *ZmMRP-1* and *Meg1* in BETL cells and a majority of zein- and starch-related genes in CSE cells. Using a haploid induction system, we show that wild-type endosperm could rescue the smaller size of *os1* embryo, which suggests that nutrients are allocated by the wild-type endosperm. Therefore, our data imply that the network regulated by OS1 accomplishes a key step in nutrient allocation between endosperm and embryo within maize seeds. Identification of this network will help uncover the mechanisms regulating the nutritional balance between endosperm and embryo.

Edited by: Bao-Cai Tan, Shandong University, China
Received Aug. 3, 2018; **Accepted** Nov. 27, 2018; **Online on** Dec. 1, 2018
FA: Free Access

Free Access

INTRODUCTION

Maize (*Zea mays* L.) is one of most important crops in the world, serving as an important food for livestock and humans (Lopes and Larkins 1993; Sabelli and Larkins 2009). The maize kernel is composed mainly of the endosperm and embryo, which are the products of double fertilization. The endosperm contributes 85% of the kernel weight and functions as a nutrient donor during embryo development and during late germination. The embryo develops inside the endosperm after double fertilization and contains in its scutellum almost all the lipids. A better understanding of the genetic mechanisms regulating endosperm and embryo development will enable approaches for genetic improvement of the maize kernel.

The endosperm is a highly differentiated organ that contains four cell types (Olsen 2001; Becraft and Gutierrez-Marcos 2012; Leroux et al. 2014). The starchy endosperm (SE) includes starch and protein, especially zein proteins. The aleurone layer (AL) is a single-cell layer surrounding the endosperm, that stores minerals and hydrolytic enzymes that are needed to metabolize the SE once it is activated during seed germination (Becraft 2001). The subaleurone layer, connects the central starch endosperm (CSE) with the aleurone, and contains several cell layers composed of zein proteins, especially γ-zeins (Geetha et al. 1991; Becraft 2001). Finally, the basal endosperm transfer layer (BETL) is important for the uptake and allocation of nutrients from maternal tissues to the endosperm and embryo (Thompson et al. 2001).

The BETL-specific protein ZmMRP-1 is a regulator that directly binds many imprinted genes with functions of nutrients allocation and BETL cell differentiation (Zhan et al. 2015). The embryo-surrounding region (ESR) plays a role in embryo development (Becraft 2001) and functions in crosstalk between the embryo and endosperm, as well as in supplying solutes to the developing embryo (Sabelli and Larkins 2009). The conducting zone (CZ) connecting the BETL with the CSE is believed to transport solutes throughout the kernel (Becraft 2001). Recently, a new cell type was identified, the basal-intermediate zone (BIZ) located between the CZ and BETL, whose function remained to be elucidated, although several marker genes have been identified (Li et al. 2014). Thousands of genes participate in the development of the different endosperm cell types (Li et al. 2014; Zhan et al. 2015); functional characterization of these genes through forward and reverse genetics will shed light on the regulatory mechanism of endosperm.

Opaque and floury endosperm mutations affect the appearance of the endosperm, often by affecting accumulation of zeins, the major endosperm storage proteins. The corresponding genes have been cloned and functionally analyzed for many of these mutations, including *o1*, *o2*, *o5*, *o7*, *o10*, *o11*, *fl1*, *fl2*, *fl3*, *fl4*, *nkd1* and *nkd2* (Zhang et al. 2018). O2 encodes a basic-domain-leucine-zipper (bZIP) transcription factor (Schmidt et al. 1987; Schmidt et al. 1990). *NKD1* and *NKD2* belong to the INDETERMINATE domain transcription factor family (Yi et al. 2015; Gontarek et al. 2016). O1 encodes a plant-specific myosin XI protein that is involved in establishment of endoplasmic reticulum (ER) structure and protein body formation (Wang et al. 2012). O5 encodes a monogalactosyldiacylglycerol synthase, and loss of function of *O5* results in galactolipid accumulation in the endosperm, leading to defects in embryo and endosperm development (Myers et al. 2011). *O7* encodes an acyl-activating enzyme that participates in amino acid synthesis (Miclaus et al. 2011; Wang et al. 2011). *O10* encodes a cereal-specific protein affecting the distribution of zeins in protein bodies (Yao et al. 2016). *Fl1* encodes an ER-located protein that affects zein protein body formation (Holding et al. 2007). Other opaque mutants, such as *fl2*, *De-B30* and *Mc*, have defects in 22-kD α-zein, 19-kD α-zein and 16-kD γ-zein proteins, respectively (Coleman et al. 1997; Kim et al. 2004; Kim et al. 2006). Moreover, RNA interference-mediated knockdown or knockout of different zeins, including the 22-kD and 19-kD α-zeins also results in opaque endosperm (Wu and Messing 2010).

The embryo forms multiple tissues and eventually develops into the mature plant. The asymmetric division of the zygote results in the apical embryo proper and suspensor, which are embedded in the ESR of the endosperm and take up nutrients via the suspensor at early developmental stages. The embryo and endosperm undergo independent and interdependent developmental processes. For example, some mutant embryos can be rescued by wild-type endosperm, and some mutant endosperms produce more or less extreme effects on wild-type embryo development (Neuffer and Sheridan 1980). Furthermore, the size of the embryo is controlled by its counterpart endosperm (Hong et al. 1996). Conversely, the embryo also affects the endosperm (Hong et al. 1996), indicating that there is a balance of resources between endosperm and embryo, although whether this involves signals, nutrients or both is unclear.

From a metabolic point of view, the embryo and endosperm are both sink organs that absorb substances from maternal tissues. However, the embryo mainly stores lipids, whereas the endosperm mainly stores carbohydrates and proteins, which make up more than 80% of the endosperm by weight. However, the nutritive interactions and any signaling between embryo and endosperm remain to be further elucidated.

In the present study, we examined the *os1* (*opaque endosperm and small germ1*) mutant and show that *OS1* encodes a putative transcription factor that regulates the development of the embryo and endosperm. The *os1* mutation results in opacity of the endosperm crown, as well as smaller embryo size. Map-based cloning showed that *OS1* encodes a RWP-RK transcription factor. RNA sequencing (RNA-Seq) demonstrated that many genes related to nutrient allocation and storage were significantly downregulated in the *os1* mutant. Moreover, the smaller size of the mutant haploid embryo could be fully rescued by wild-type, but not mutant, endosperm, *in vivo*. Overall, our data show that OS1 is required for nutrient allocation between embryo and endosperm owing to its regulation of downstream genes.

RESULTS

Maize *os1* mutant has opaque endosperm and a smaller embryo

The *os1* mutant was identified in 1993 and characterized as having opaque endosperm and a smaller embryo, compared with wild type (Song and Lu 1993). Upon backcrossing *os1* to the M017 inbred line, we observed no phenotypic differences in the mature ears between homozygous mutant and wild-type plants, in regard to ear length, diameter or number of rows (Figures 1A, S1). Further analysis of the kernel phenotypes revealed that the mutant has a smaller embryo (Figure 1B lines 1 and 2) and opaque endosperm crown (Figure 1B line 3). In cross-sections, the *os1* mutant showed a starchy endosperm, and a small cavity also developed in the mutant kernel (Figure 1B lines 4 and 5).

The opaque and smaller embryo phenotypes were tightly linked in contrast to other maize opaque mutants. Moreover, many opaque mutants, such as *o2*, *o1*, *o5*, *o7* and *o11*, have reduced kernel weight, but we saw no significant difference in seed weight between *os1* and wild-type M017 (Figure 1C, top). However, the mutants had increased endosperm weight (Figure 1C, middle), but significantly decreased embryo weight and size (Figure 1C, bottom).

Maize *os1* mutant has altered zein and non-zein protein content

To investigate the potential causes of the opaque endosperm and smaller embryo in *os1*, we analyzed the texture and nutritional composition of the endosperm and embryo in mature seeds of *os1* and wild-type. Scanning electron microscopy of the upper endosperm indicated that the *os1* mutant exhibited a floury endosperm in the peripheral and central regions, whereas wild-type seeds had a vitreous endosperm (Figure 2A, B). Developmental defects of the aleurone and subaleurone cell layers have been observed in the kernel mutant *nkd1 and nkd2* (Li et al. 2015; Gontarek et al. 2016). In contrast to wild type (Figure 2C), we observed that in the *os1* mutant, the subaleurone cell layers were not visible, being replaced by starchy cells, which resulted in tight contact between the starchy cells and the aleurone cell layer (Figure 2D).

Changes in nutrient composition are key causes for endosperm opacity (Zhang et al. 2018). We therefore compared the compositions of zein and non-zein proteins between mature seeds from *os1* and M017. We divided the endosperm into two halves (upper and lower, as shown in Figure 1B line 1). We found that the levels of almost all zein proteins, especially 27-kD γ-zein and 22-kD and 19-kD α-zein, were sharply decreased in the endosperm of *os1* as compared to wild-type seeds (Figure 3A). These differences were more obvious in the upper than in the lower endosperm. For the non-zein proteins, we also found four bands that were sharply decreased in the *os1* mutant (Figure 3B). Interestingly, two unknown non-zein-protein bands were increased in the *os1* mutant (Figure 3B).

We also performed transmission electron microscopy of the protein bodies, using upper endosperm near the top pericarp obtained at 18 d after pollination (DAP). The *os1* mutant had smaller starch granules (Figure 3C, D) and sparser protein bodies (Figure 3E, F) as compared to the wild type. These results suggested that nutrient deposition in the endosperm is unbalanced in the *os1* mutant.

Nutritional composition of the endosperm and embryo is altered in the *os1* mutant

To further define the unbalanced nutrient composition of the *os1* mutant endosperm, we next performed comparative nutrient measurements of the mutant and wild type to determine carbohydrate and crude protein levels in embryo and endosperm, as well as amino acid and oil levels in the whole kernel. For carbohydrates, we observed significant increases in mutant kernels but no differences in endosperm (Figure 4A). The mutant embryos also accumulated more crude protein, per gram, than the wild-type embryos, but no differences were seen in the kernel or endosperm (Figure 4B). In regard to oil content, we observed sharp decreases of total seed oil content and the primary oil components of C16:0, C18:1 and C18:2 in embryo in the *os1* mutant compared with wild type, which was in line with the smaller embryo of the mutant (Figure 4C).

We also measured the contents of 18 amino acids in mature kernel, embryo and endosperm. The results indicated that six and four amino acids were significantly less abundant in the mutant kernel and endosperm, respectively, as compared to wild-type seeds. Only one amino acid was more abundant in mutant kernel and three were more abundant in

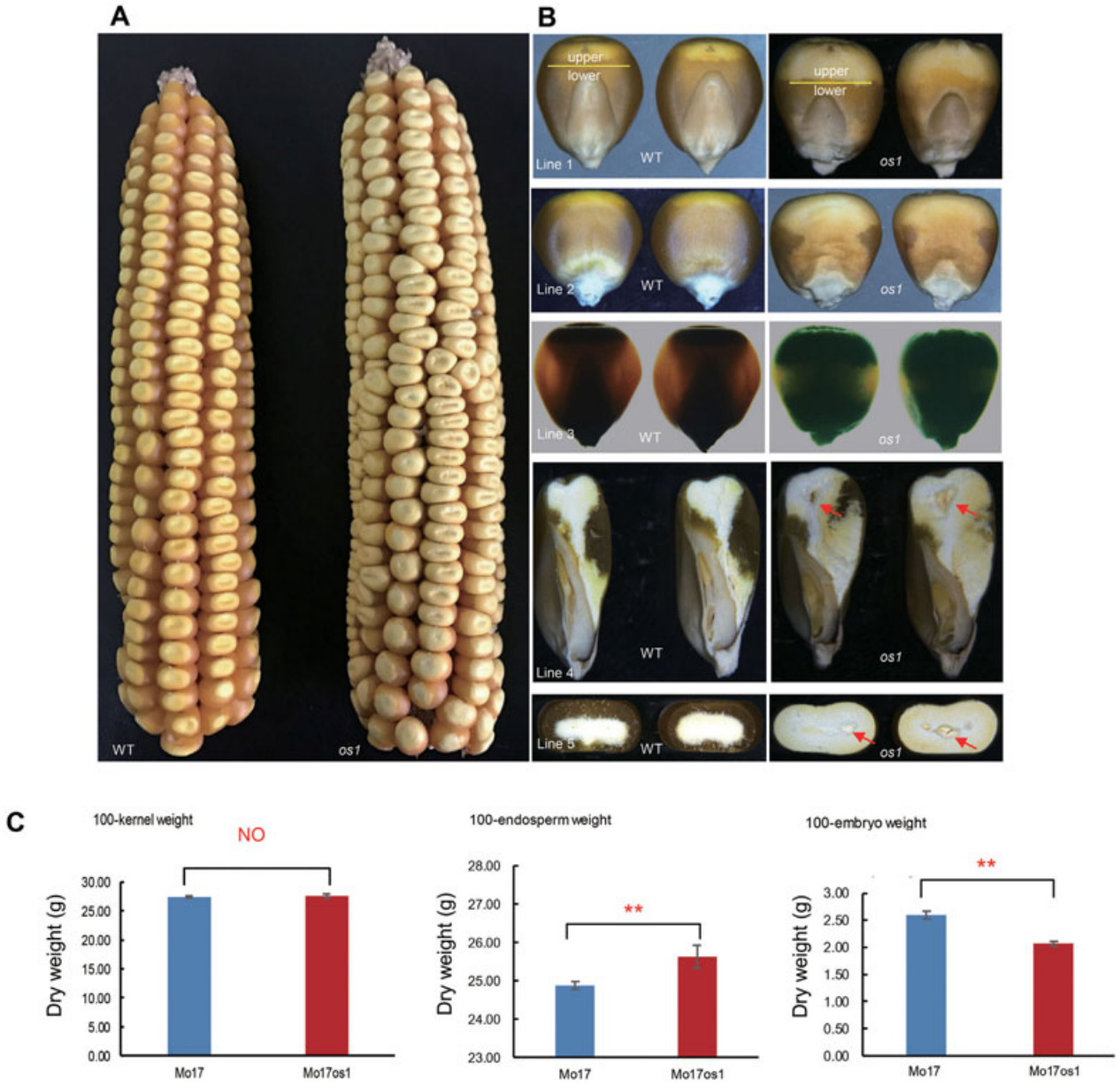

Figure 1. Phenotypic analysis of the *os1* mutant

(A) Homozygous ear phenotype of wild type (Mo17; left) and *os1* mutant (Mo17*os1*; right). **(B)** Kernel phenotypes of wild type (left) and *os1* (right). Line 1, adaxial face of kernel; line 2, abaxial face of kernel; line 3, light transmission of kernel; line 4, longitudinal sections; line 5, transverse sections. Red arrows indicate cavity in endosperm. The kernels were marked as upper and lower part of seed by using a yellow line on the kernel. **(C)** Comparisons of the weights of 100-kernel (top), 100-endosperm (middle) and 100-embryo (bottom) between wild type and *os1*. Values are mean ± *SD* ($n = 100$). Two stars represent $P < 0.01$, one star represents $P < 0.05$.

mutant endosperm (Figure 4D, E). However, the majority of amino acids (14 out of 18) were significantly more abundant in the embryo of the mutant as compared to the wild type (Figure 4F). Taken together, these data suggest that in the mutant seeds, the allocation of nitrogen and carbohydrate is unbalanced between the embryo and endosperm.

Map-based cloning of *OS1*

The causative gene of *os1* was initially mapped, cytogenetically, to the short arm of chromosome 2

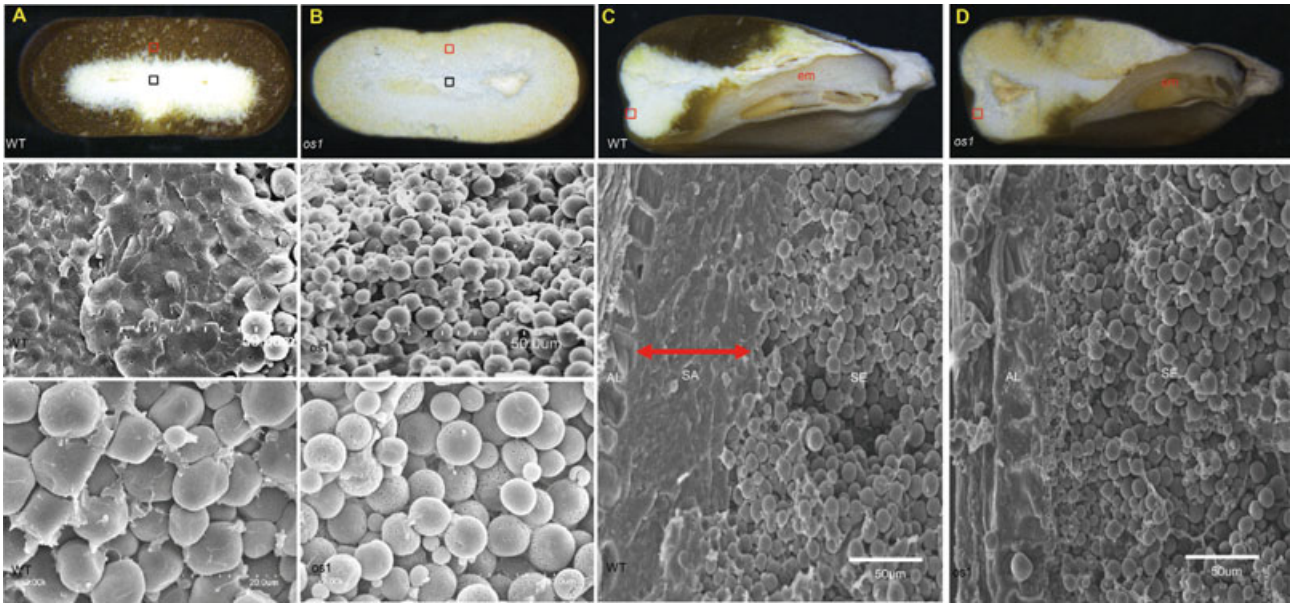

Figure 2. Characterization of starchy endosperm in *os1* and wild type at the mature kernel stage
(A, B) Scanning electron microscope (SEM) analysis of starch granules in peripheral (red box) and central (black box) regions of mature endosperm of wild type (M017; **A**) and *os1* mutant (M017*os1*; **B**) kernels. Top, transverse sections of kernels; middle and bottom, kernel peripheral regions (scale bars = 50 μm [middle] and 20 μm [bottom]). **(C, D)** SEM analysis of starch granules in peripheral (red box) mature endosperm of wild type (**C**) and M017*os1* kernels (**D**). Top, longitudinal sections of kernels. Bottom, kernel crown regions (scale bars = 100 μm [top] and 50 μm [bottom]). AL, aleurone cells; SA, sub-aleurone layers; SE, starch endosperm.

(Song and Lu 1993). To clone *OS1*, we crossed the *os1* mutant with M017. Then we focused on the short arm of chromosome 2 and mapped the *OS1* locus to the bin 2.03 region between two simple sequence repeat (SSR) markers, umc1845 and umc2193, by using 93 BC1F1 individuals (Figure 5A). For fine mapping of *OS1*, we screened 3,252 BC1F1 individuals and developed an additional 10 molecular markers (P1–P10) (Figure 5B; File S1). Finally, we narrowed down the target interval to a 250 kb region flanked by the P7 and P9 markers in the BAC clones of AC210203 and AC1940411, respectively.

According to the annotation information, three candidate genes were predicted within the 250 kb region (Figure 5C). Sequence analysis revealed a 3.5 kb *hAT* transposon insertion in the predicted RWP-RK transcription factor in the mutant *os1*. Alignment of the cDNA and genomic DNA sequences revealed that the gene contains five exons and four introns and that the insertion occurred in the second exon (Figure 5D). Finally, results from a reverse transcription quantitative PCR (RT-qPCR) analysis suggested that the putative RWP-RK transcription factor was the strongest candidate for *OS1* (Figure 5E).

Functional complementation of *OS1* by allelism test and maize transformation

To confirm that disruption of the candidate gene caused the mutant phenotype, we set out to isolate another allele by screening a *Mu*-transposon-based mutant library. We ultimately isolated an allele that we named *os1-mu1*. Sequence analysis revealed that this mutant contains a 1.3 kb *Mu1* transposon insertion in the second exon of the gene encoding an RWP-RK transcription factor (Figure S2A, B). To test the allelic relationship between *os1* and *os1-mu1*, we reciprocally crossed the two mutants. All the seeds on the cross-pollinated ears (F1) showed an opaque, small embryo phenotype (Figure S2C).

In addition, we developed a maize transformation test for the candidate RWP-RK transcription factor. We cloned the 7.0 kb genomic sequence containing its entire gene body into the multiple cloning site of the vector pCAMBIA3301. We then transformed the construct into the immature embryos from the F_1 plants of HiIIA × *os1* using the *Agrobacterium tumefaciens* strain EHA105. Five transgenic events were generated and self-pollinated and the kernels on the resulting ears

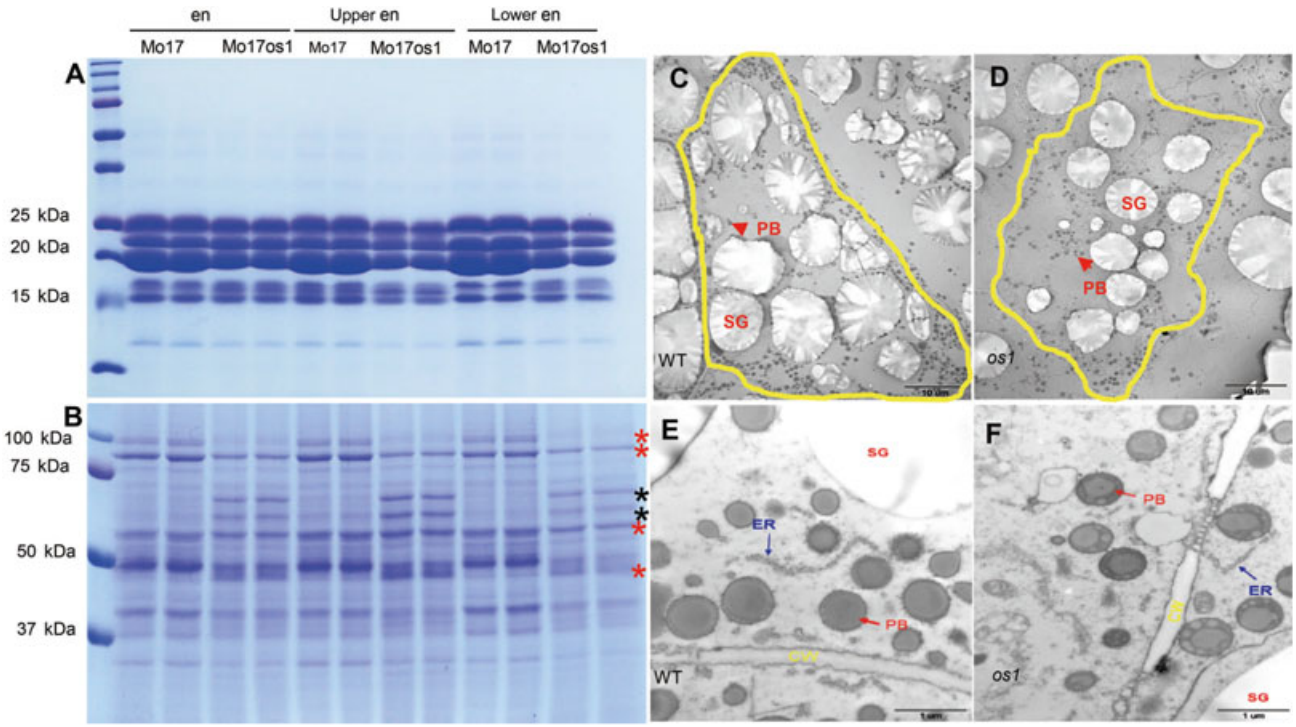

Figure 3. Characteristic analysis of zein and non-zein proteins and transmission electron microscopy (TEM) analysis of regions in maize kernels

(A) Zein proteins extracted from endosperm (en), upper endosperm (upper en) and lower endosperm (lower en), respectively. **(B)** Non-zein proteins extracted from total endosperm, upper endosperm and lower endosperm, respectively. Red stars represent decreased bands, black stars represent increased bands in the mutant endosperm. **(C)** Starch granules in a starchy cell of wild type Mo17. **(D)** Starch granules in a starchy cell of *os1* mutant. **(E)** Protein bodies in starchy cells of wild type Mo17. **(F)** Protein bodies in starchy cells of *os1* mutant. Scale bars = 10 μm (**C**, **D**) and 1 μm (**E**, **F**).

were scored in the T1, and 15:1 segregation ratios for wild type: mutant phenotype (Table S1) were observed in three events. This showed that the *os1* mutant phenotype could be functionally complemented by the introduced transgenic allele. Taken together, these data strongly supported the hypothesis that a 3.5 kb *hAT* transposon insertion in *OS1* in the *os1* mutant cause the phenotype of opaque endosperm and smaller-size embryo.

OS1 encodes a putative RWP-RK domain-containing transcription factor

OS1 encodes a putative RWP-RK domain-containing transcription factor with bipartite SV40-like nuclear localization signals (Schauser et al. 1999), and one of these family members was also functionally analyzed in *Arabidopsis* (*Arabidopsis thaliana*) (Castaings et al. 2009). *OS1* is predicted to be a member of the RWP-RK-domain (RKD) subfamily of transcription factors. Full-length OS1 contains 331 amino acids, with the conserved RWP-RK domain spanning approximately 55 amino acids. Phylogenetic analysis of full-length OS1 homologs from monocotyledonous and dicotyledonous species classified these into two major clades (Figure 6A; File S2). OS1 was grouped into the RKD clade, along with AtRKD4 and AtRKD5, which are involved in embryo development (Jeong et al. 2011; Waki et al. 2011; Tedeschi et al. 2017) (Figure 6A).

To investigate the subcellular localization of the protein, we amplified the full-length cDNA of *OS1* from the elite inbred maize line B73 and cloned it into a vector containing the green fluorescent protein (GFP) reporter gene and bombarded this construct into onion cells (Figure 6B, C). We observed signals from the control construct containing only *GFP* in the cytoplasm and all organelles, including the cell nucleus (Figure 6D–F), but

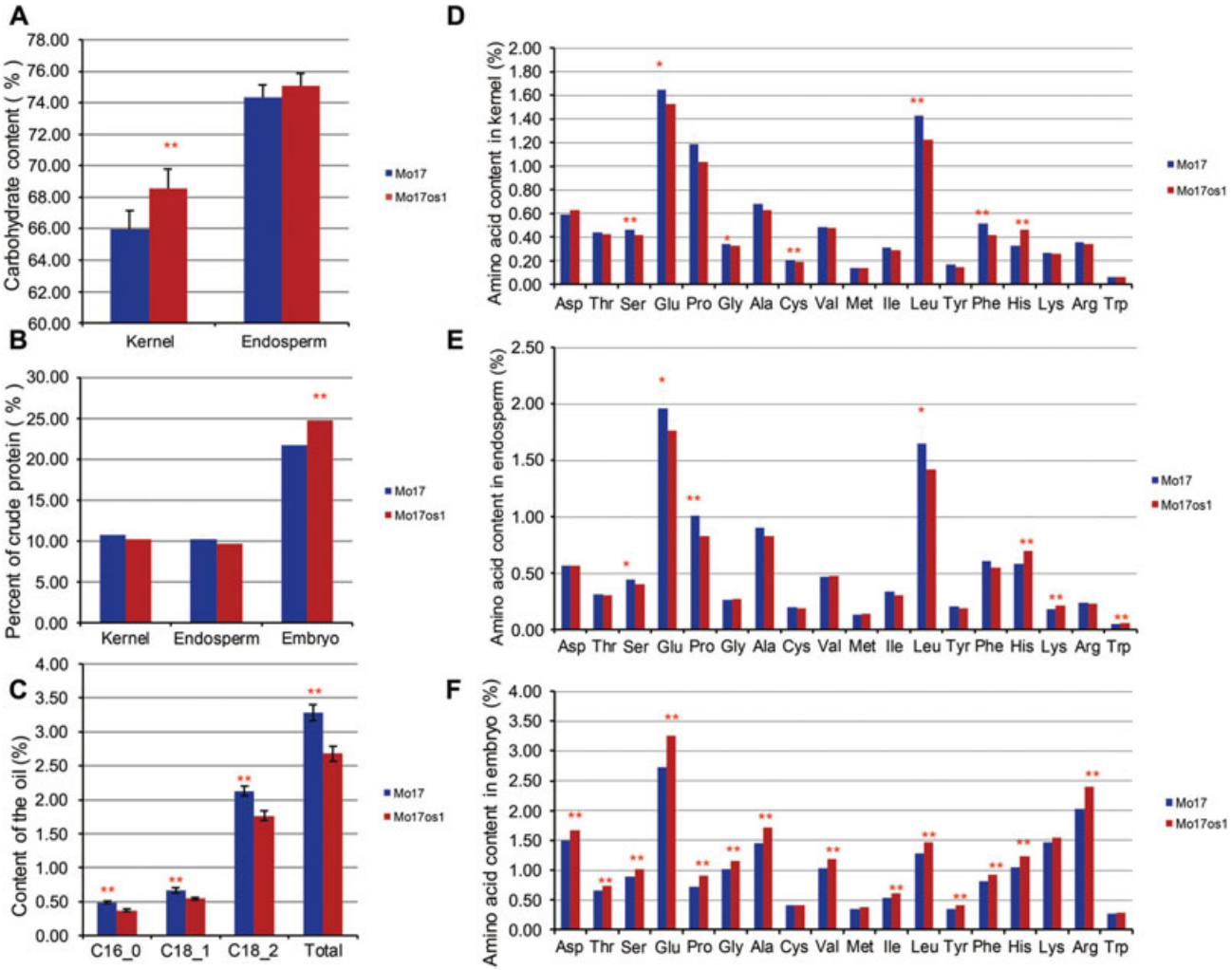

Figure 4. Measurement of different nutrient components in the mature kernel, endosperm and embryo of mutant (Mo17*os1*) and wild type (Mo17) maize kernels

(A) Total carbohydrate content in the kernel and endosperm. **(B)** Crude protein content in the kernel, endosperm and embryo. **(C)** Total oil content and main components of oil in the kernel. **(D–F)** Eighteen amino acids from the kernel (**D**), endosperm (**E**) and embryo (**F**) between the mutant and wild type. Values are mean ± *SD* ($n = 120$). Two stars represent $P < 0.01$, one star represents $P < 0.05$.

the fused protein was detected only in the nucleus (Figure 6G–I).

We further transformed the *OS1 GFP* fusion into maize and examined the fluorescence of the juvenile leaf epidermis of the maize transgenic plants to detect OS1's localization in maize cells. Whereas the control unfused GFP localized to various organelles (Figure 6J, L), the fused protein was detected only in the nucleus (Figure 6M–O). These results indicated that the OS1 protein contains nuclear localization signals, which is consistent with a function as a transcription factor. However, we did not find any transcriptional activation activity of OS1 via yeast one-hybrid system (Figure S3).

Expression pattern of *OS1*

We performed semi-quantitative RT-PCR analysis to investigate the expression pattern of *OS1* gene in the kernel, tassel, ear, leaf, and other tissues. The results showed that *OS1* is expressed in all 10 tissues analyzed, implying that it is constitutively expressed in maize (Figure 7A). Among the 10 tissues, the highest *OS1* expression was detected in ear (Figure 7A). Based on the *os1* mutant phenotype of opaque endosperm and small embryo, we investigated the expression of *OS1* in

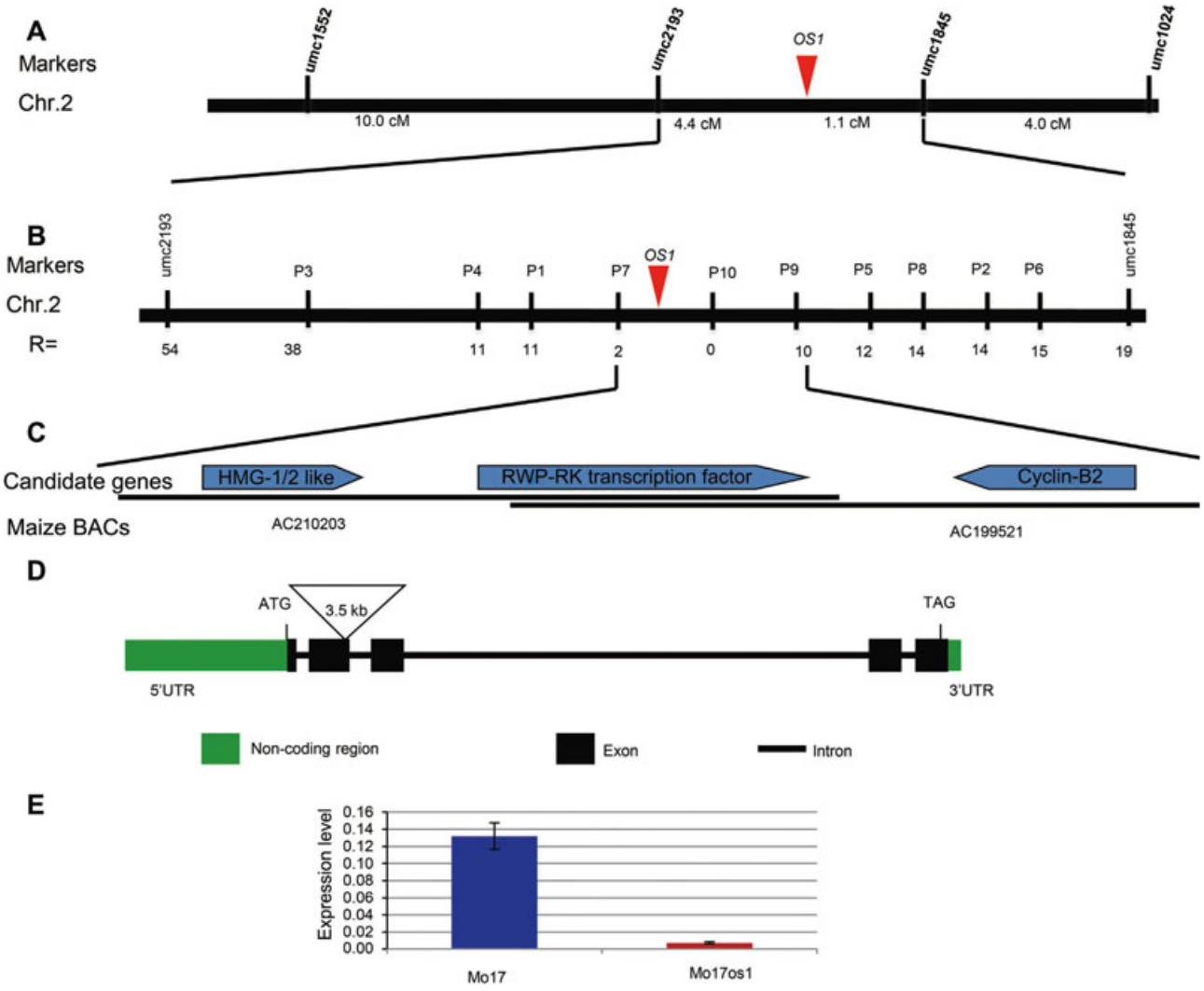

Figure 5. Map-based cloning of the maize *OS1* gene

(A) Genetic mapping of *OS1* using the BC1F1 population. *OS1* is located in the 5.5-centiMorgan (cM) interval between the SSR markers umc2193 and umc1845 on chromosome 2. **(B)** Location of *OS1* was narrowed down to a small genomic region (a physical interval of 250 kb) between markers P7 and P9. **(C)** Three candidate genes were identified, as sequence analysis revealed three candidate genes in the region. R, recombinant. **(D)** Sequencing and comparison of the genomic DNA and cDNA sequence between mutant line *os1* and the inbred line B73 reveals a 3.5 kb insertion present in the second exon of the mutant line. **(E)** qRT-PCR analysis of *OS1* expression from Mo17 and Mo17*os1* maize lines.

the endosperm, embryo and kernel using our previously published data (Chen et al. 2014).

Generally, the expression of *OS1* showed greater variation over the course of development in the endosperm than in the embryo. *OS1* expression in endosperm peaked at 6 DAP and then declined until 38 DAP (Figure 7B). Furthermore, investigation of laser-capture microdissection (LCM) data from 8-DAP seed revealed that *OS1* exhibited higher expression levels in the CSE, CZ and BETL among the different cell types in endosperm (Zhan et al. 2015). Taken together, these results suggest that *OS1* expresses in endosperm mainly at earlier developmental stages, during the period of vigorous differentiation of endosperm.

To investigate the expression pattern of *OS1* among the different cell types of the developing kernels at earlier stages, we performed in situ hybridization using 4-, 6-, 8- and 10-DAP kernels, which include the differentiation stages of the endosperm as well as post-differentiation stages (File S3). Our results revealed

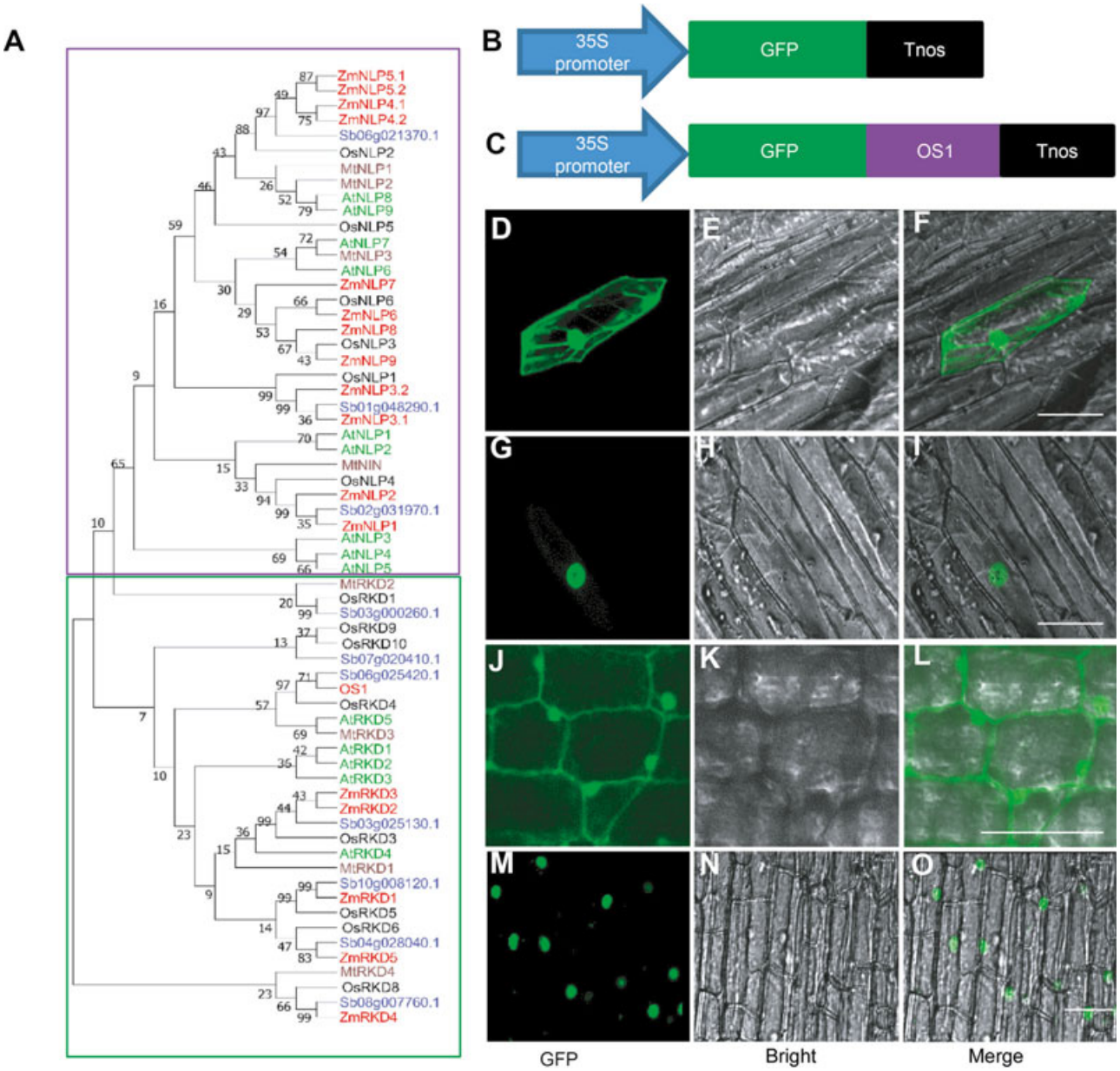

Figure 6. Subcellular localization and phylogenetic analysis of plant RWP-RK domain-containing proteins

(A) Phylogenetic tree (obtained using MEGA 5.0) of the RWP-RK-domain-containing proteins sequences from maize, rice, *Arabidopsis*, sorghum and *Medicago sativa* L. Sequences were downloaded from Chardin et al. (2014) and aligned using Clustalw. Zm, *Zea mays*; At, *Arabidopsis thaliana*; Os, *Oryza sativa*; Sb, *Sorghum bicolor*; NLP, Nin-like protein; RKD, RWP-RK domain. Red indicates maize accessions, black indicates rice, green indicates *Arabidopsis*, blue indicates sorghum and light purple indicates *Medicago sativa*, the purple and green regions represent the NLP and RKD groups, respectively. **(B, C)** Construction of control *GFP* vector (**B**) and *GFP-OS1* fusion protein vector **(C)**. **(D–F)** Subcellular localization of GFP protein in epidermal cells of onion transformed with control vector. **(G–I)** Subcellular localization of OS1 protein in epidermal cells of onion transformed with the fusion protein vector. **(J–L)** Subcellular localization of control vector containing GFP protein in epidermal cells of a maize leaf. **(M–O)** Subcellular localization of OS1 protein in epidermal cells of a maize leaf. For each group, location signal is indicated by the GFP fluorescence (green) in the left column. The cells are indicated by the bright field in the middle columns. The merged views are shown in the right column. Bars = 50 μM.

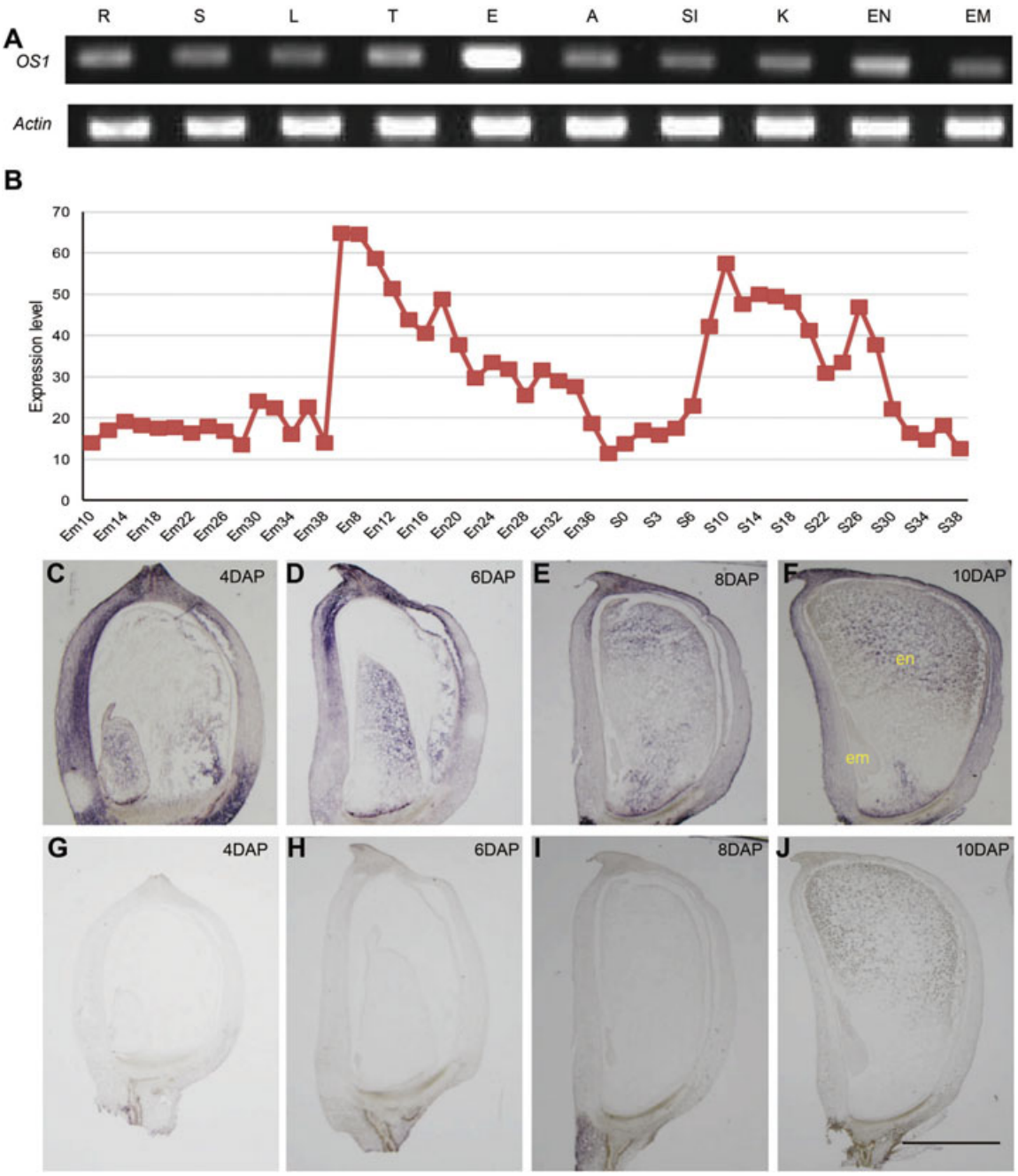

Figure 7. Expression patterns of the *OS1* gene

(A) RT-PCR analysis of *OS1* expression in 10 different tissues: R, root of 2-week-old field-grown seedling; S, shoot of 2-week-old filed-grown seedling; L, leaf of 2-week-old filed-grown seedling; T, 5 cm tassel; E, 5 cm immature ear; A, anther; SI, 5-cm silk emerged from ear before pollination; K, 16-DAP kernel; EN, 16-DAP endosperm; EM, 16-DAP embryo. **(B)** Expression pattern of *OS1* in different tissues derived from the expression data reported by Chen et al. (2014). **(C–F)** RNA *in situ* hybridization of *OS1* in developing seeds. Longitudinal sections of kernels at (left to right) 4, 6, 8 and 10 d after pollination (DAP) were hybridized with an antisense RNA probe for *OS1*. Positive signals (blue-violet) for *OS1* were observed primarily in the basal endosperm transfer layer (BETL), conducting zone (CZ) and central starch endosperm (CSE) in endosperm, but not in the embryo. **(G–J)** Longitudinal sections of B73 kernels at 4, 6, 8 and 10 DAP hybridized with a sense RNA probe for *OS1*. No signals were detected in the corresponding sections. em, embryo; en, endosperm. Scale bar = 1.5 mmol/L.

that the expression of *OS1* was widely distributed within seeds. In the endosperm, strong signals were detected in the BETL, CZ and CSE cell types (Figure 7C–J), which was consistent with the expression patterns identified from the LCM data (Zhan et al. 2015). At all four stages analyzed, we could not detect any signals in embryo, indicating that *OS1* functions mainly in endosperm.

RNA-Seq analysis of endosperm

To identify the regulatory processes in which *OS1* is involved, we performed a transcriptome analysis between mutant and wild-type. Considering that *OS1* showed its highest expression at 6 DAP, and that the abundances of multiple zein proteins were declined in the *os1* mutant at mature stages, we used 6- and 14-DAP endosperm for the transcriptome analysis. In total, we obtained 21.8 and 26.8 million paired-end reads for 6-DAP endosperm and 20.6 and 23.4 million reads for 14-DAP endosperm from mutant and wild type, respectively, from two biological repeats.

Among these, we identified 845 and 1,247 differentially expressed genes (DEGs) at 6-DAP and 14-DAP, respectively, in the *os1* mutant as compared to the wild type (File S4). We identified 522 downregulated genes and 323 upregulated genes at 6 DAP, and 688 downregulated genes and 559 upregulated genes at 14 DAP (Figure 8A–D). Among the DEGs detected at 6 DAP, *ZmMRP-1* (GRMZM2G111306), encoding a well-known regulator of BETL differentiation and function (Zhan et al. 2015), showed significantly decreased expression in the *os1* mutant. Furthermore, we determined that four direct target genes of ZmMRP-1, *meg1*, *meg2*, *meg6* and *meg15*, were significantly downregulated at 6 DAP. Finally, we found 31 DEGs encoding proteins related to plant defense, protease inhibitors, as well as basal layer antifungal protein (BAP) and imprinted genes, that are highly expressed in BETL and ESR cells and have functions in nutrient uptake and allocation within seeds (Figure 8E; File S5).

At the 14-DAP time point, 26 genes related to synthesis of zeins and starch were preferentially expressed in CSE cells (Figure 8E), which is consistent with the significantly reduced abundances of multiple zeins in *os1* mutant endosperm. These results suggested that OS1 might directly or indirectly regulate these genes related to nutrient reservoirs. Further gene ontology (GO) analysis revealed that the terms "defense response" and "peptidase activities" were enriched among DEGs at 6 DAP, whereas the term "nutrient reservoir activity" was most highly enriched at 14 DAP (Table 1).

To validate the RNA-Seq data, we selected 24 DEGs that were either downregulated or upregulated at the 6- and 14-DAP time points to be further tested by RT-qPCR. In all cases, the RT-qPCR data strongly agreed with the corresponding variation patterns in the RNA-Seq data (Figure 8F–I), confirming the reliability of our RNA-Seq data.

Wild-type endosperm rescues the mutant embryo, *in vivo*

The combination of decreased embryo weight, increased endosperm, but no difference in kernel weight, implied that nutrient allocation between endosperm and embryo is unbalanced within the mutant seeds. In addition, the RNA-Seq data indicated that many genes involved in nutrient allocation and transport as well as nutrient reserve maintenance were downregulated in mutant. These included *Meg1*, which encodes an imprinted maternally expressed gene; Mn1, which encodes a cell wall invertase; the gene encoding the 27-kD zein protein; and so forth. Furthermore, it has also been reported that imprinted genes play important roles in nutrient allocation between endosperm and embryo after double fertilization. Finally, *in situ* hybridization in the endosperm also showed that *OS1* preferentially expresses in cell types that are responsible for nutrient uptake and transport (Figure 7). For all of these reasons, we inferred that nutrient allocation between embryo and endosperm within seeds might be unbalanced in the *os1* mutant.

We then performed crosstalk analysis of different genotypes between embryo and endosperm using the double haploid system in two genetic backgrounds of os1 (original *os1* mutant inbred line with unknown background) and Mo17. We crossed the mutant (as a maternal parent) with mixed pollen of the double haploid line CAU05 and the corresponding mutant line (as a paternal parent).

After pollination, we obtained three types of seeds in the same ear: seeds with both the endosperm and embryo mutant (endosperm/embryo: *os1 os1 os1*/ *os1 os1*), diploid seeds with both the endosperm and embryo wild type (endosperm/embryo: *os1 os1 OS1*/ *os1 OS1*), and haploid seeds with wild-type endosperm and haploid embryo (endosperm/embryo: *os1 os1 OS1*/ *os1*) (Figure 9A). Interestingly, we determined that the

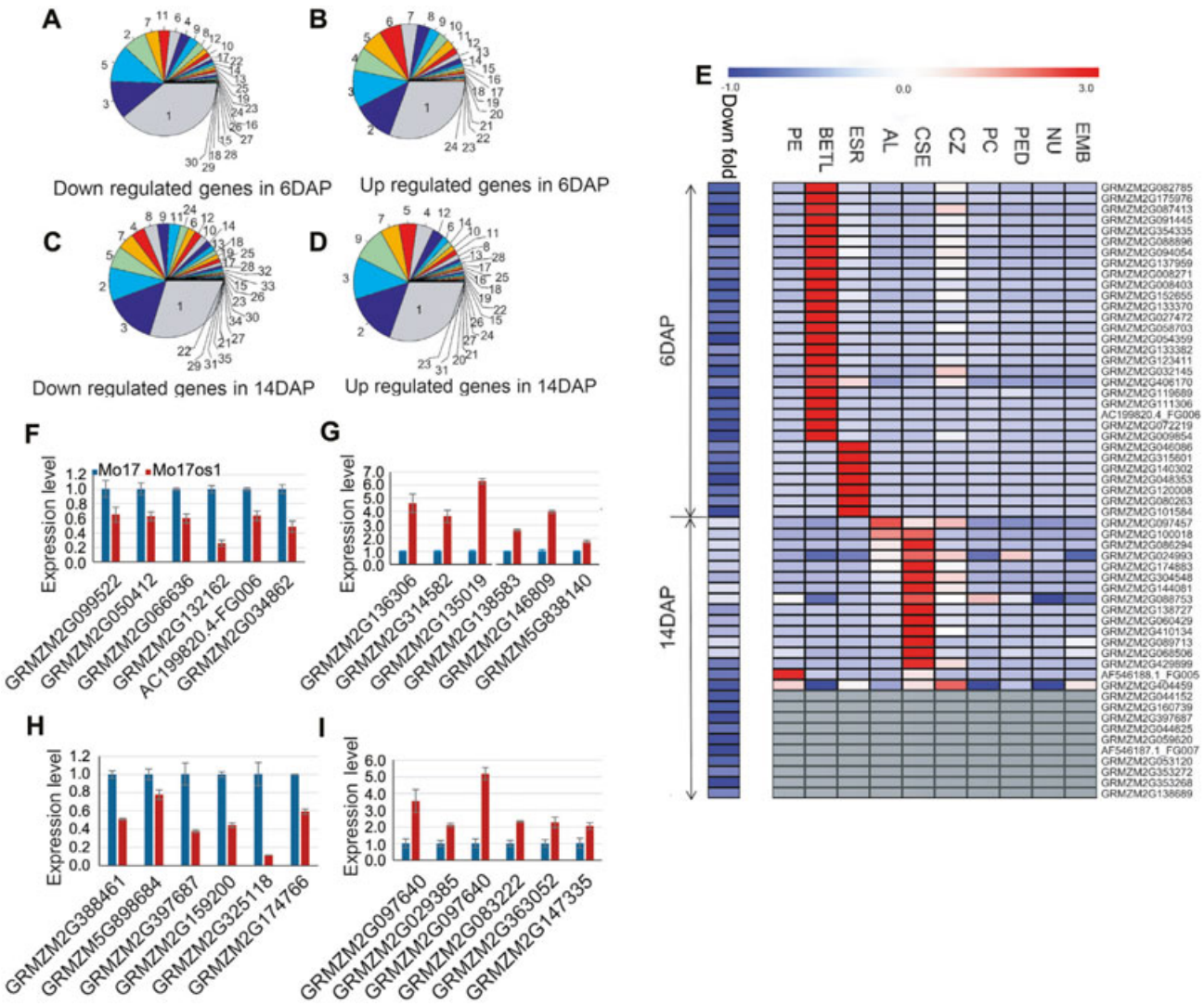

Figure 8. Transcriptome comparison between *os1* mutant and wild-type maize endosperm using RNA-Seq

(A–D) Functional categories of the DEGs in *os1* mutant using MapMan among genes downregulated (**A**) and upregulated (**B**) at 6 DAP and downregulated (**C**) and upregulated (**D**) at 14 DAP. **(E)** Heat map of the downregulated genes associated with nutrient allocation and nutrient reserves in the endosperm, as determined from RNA-Seq data. Genes downregulated in the *os1* mutant were selected from RNA-Seq data of 6-DAP and 14-DAP endosperm. Heat map on the left shows the fold change for the downregulated genes in the *os1* mutant, as compared with wild type. Heat map on the right was drawn based on the data of Zhan et al. (2015). Gene IDs are shown to the right of the heat map. AL, aleurone; BETL, basal endosperm transferring layer; CSE, central starch endosperm; CZ, conducting zone; EMB, embryo; ESR, embryo-surrounding region; NU, nucellus; PE, pericarp; PED, pedicel; PC, placento-chalazal region. RT-qPCR validation of the selected DEGs: genes that were downregulated (**F, H**) and upregulated **(G, I)** at 6-DAP and 14-DAP time points, respectively. Zmubiquitin was used as an internal reference. Values are mean ± *SD* ($n = 3$).

wild-type endosperm could almost rescue the small embryo to a wild-type phenotype, in regard to size, weight (Figure 9B, C) and oil content (Figure 9D) in haploid seeds in comparison with diploid mutant seeds.

First, we compared seed-related parameters between the three types of seed; these included embryo length (EL), kernel length (KL), embryo weight (EW) and kernel weight (KW), as well as the ratios EL/KL and EW/KW, in the two genetic backgrounds (Figure 9B; top is *os1* original inbred line background and bottom is Mo17 background). We identified significant differences in EL, EW and EL/KL between haploid and mutant seeds, as well as diploid wild-type seeds and mutant-type seeds, in both

Table 1. GO term annotations of the transcriptomes at the 6-DAP and 14-DAP time points

GO term	Description	Number in input list	Number in BG/Ref	*P*-value	FDR	Time point
GO:0006952	defense response	26	608	3.10E-07	0.00035	6-DAP
GO:0006629	lipid metabolic process	34	1,068	3.40E-06	0.0019	
GO:0006665	sphingolipid metabolic process	6	39	2.40E-05	0.0088	
GO:0006643	membrane lipid metabolic process	6	46	5.60E-05	0.015	
GO:0016798	hydrolase activity, acting on glycosyl bonds	32	821	1.00E-07	5.90E-05	
GO:0016787	hydrolase activity	121	6,078	1.40E-06	0.00039	
GO:0004553	hydrolase activity, hydrolyzing O-glycosyl compounds	27	767	6.30E-06	0.0012	
GO:0005507	copper ion binding	11	194	8.10E-05	0.012	
GO:0070001	aspartic-type peptidase activity	12	259	0.00024	0.023	
GO:0004190	aspartic-type endopeptidase activity	12	259	0.00024	0.023	
GO:0070011	peptidase activity, acting on L-amino acid peptides	36	1,493	0.00045	0.037	
GO:0000156	two-component response regulator activity	6	75	0.00065	0.039	
GO:0009055	electron carrier activity	25	914	0.00062	0.039	
GO:0008233	peptidase activity	36	1,529	0.00069	0.039	
GO:0005764	lysosome	5	25	3.80E-05	0.002	
GO:0000323	lytic vacuole	5	25	3.80E-05	0.002	
GO:0005773	vacuole	5	38	0.00023	0.0079	
GO:0045735	nutrient reservoir activity	21	146	8.90E-16	5.30E-13	14-DAP
GO:0042579	microbody	5	33	7.80E-05	0.0055	
GO:0005777	peroxisome	5	33	7.80E-05	0.0055	

backgrounds, but no differences in KL, KW or EW/KW. These results suggested that the weight and length of mutant embryo in the haploid (*os1 os1 OS1*/*os1*) were rescued or restored to normal levels by wild-type endosperm with the genotype of *os1 os1 OS1*.

Second, we measured the area of the embryo axis side and the oil content of the whole kernel in all three types of seeds. Both the area and the oil content of the haploid embryo were the same as those of the diploid in both backgrounds (Figure 9C, D), indicating that the mutant embryo was successfully rescued by wild-type endosperm *in vivo*.

Taken together, we propose a working model for the function of *OS1* during seed development (Figure 9E). After undergoing double hybridization, the zygote starts the first cell division (which will be followed by multiple cell propagations) by embedding in the endosperm. Then, the embryo needs the endosperm to provide nutrients via OS1 by regulating genes related to resource transportation, allocation and reserve maintenance between embryo and endosperm (Figure 9E, upper). Loss of function of *OS1* results in decreased accumulation of zein proteins in endosperm and of lipids and other nutrients in embryo leading to unbalanced nutrients allocation within seed (Figure 9E, lower), implying that OS1 has an important regulatory role during the development of endosperm and embryo.

DISCUSSION

Maize *os1* is a new opaque mutant

As easily detectable phenotypes, mutants with opaque or floury endosperm have been identified, characterized and functionally elucidated. Generally, these mutants have been grouped into several classes, based on their phenotypes: first, mutants with opaque endosperm and decreased seed weight but normal seed size, such as *o2*, *o7* and *nkd* (Schmidt et al. 1987; Wang et al. 2011; Yi et al. 2015; Gontarek et al. 2016); second, those with opaque

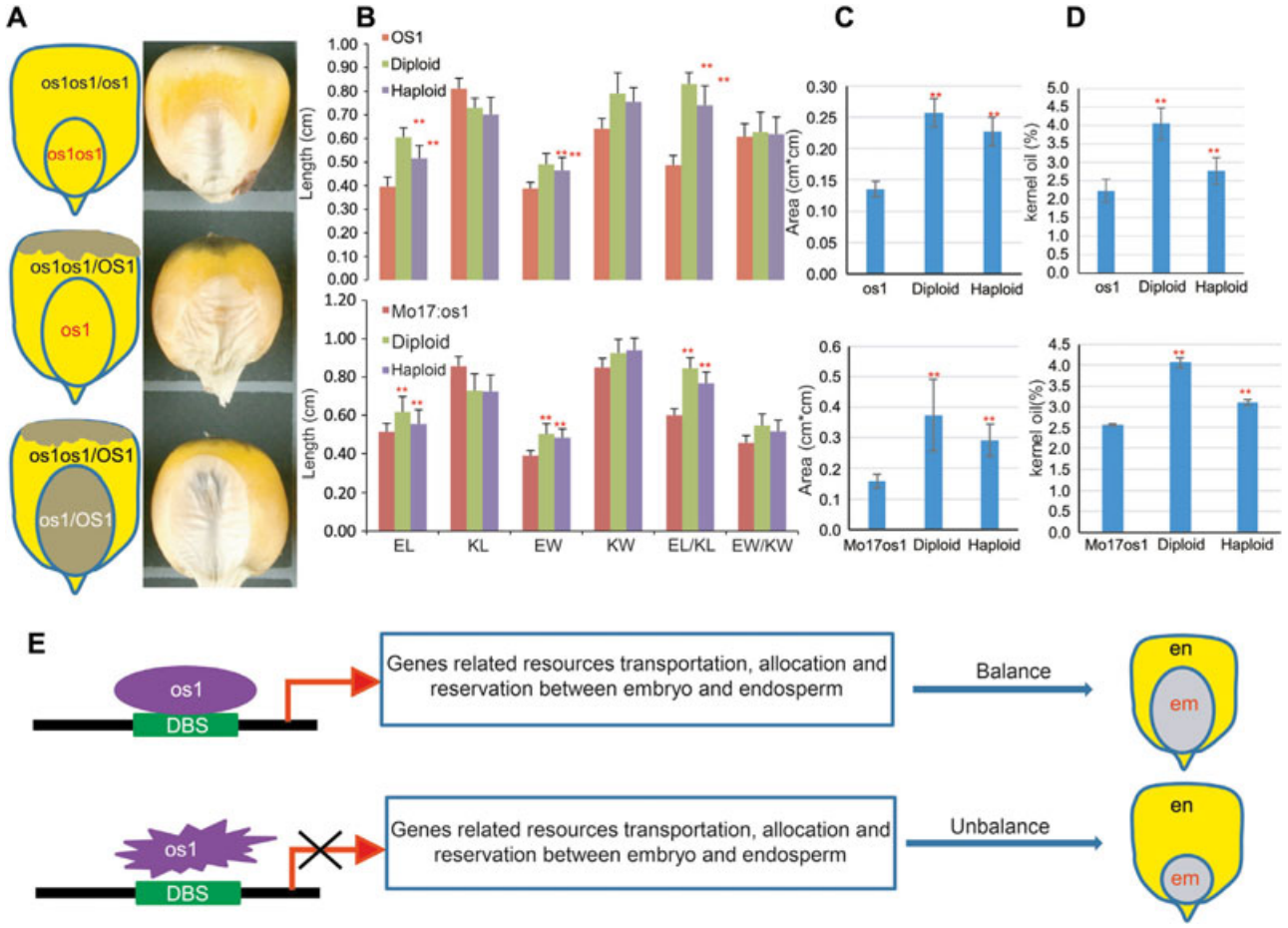

Figure 9. Rescue of the *os1* small embryo size phenotype by wild-type endosperm via haploid induction
(A) Crosses of *os1* and Mo17os1 with the haploid inducer CAU5 yielded two types of kernel: haploid and diploid. **(B–D)** Sizes (**B**), embryo areas **(C)** and oil contents **(D)** of different types of kernels. EL, embryo length; EL/KL, embryo length/kernel length; EW, embryo width; EW/KW, embryo width/kernel width; KL, kernel length; KW, kernel width. Values are mean ± *SD* ($n = 90$). **(E)** Proposed working model of *OS1* function in the maize kernel. *OS1* functions as a nutrient allocator between the endosperm and embryo. In wild type, *OS1* regulates multiple genes involved in nutrient allocation and metabolism, resulting in normal endosperm and embryo (upper). In the *os1* mutant, the targets of *OS1* are downregulated, producing a smaller embryo and opaque endosperm (lower).

endosperm and decreases in both seed size and seed weight, such as *o5*, *o11* and *floury3* (Myers et al. 2011; Li et al. 2017; Feng et al. 2018); third, those with opaque endosperm and misshapen protein bodies but no alteration of zein or non-zein protein contents, such as *o1* and *o10* (Wang et al. 2012; Yao et al. 2016); and fourth, those with opaque endosperm and both misshapen protein bodies and decreased zein content, such as *floury2*, *Mucronate* (*Mc*) and *DeB30* (Coleman et al. 1997; Kim et al. 2004; Kim et al. 2006).

These opaque mutants exhibit typical opacity across the whole endosperm without any effect on the development of the corresponding embryo. Our data for the *os1* mutant revealed that it has decreased zein protein contents, typical for opaque mutants, but in other regards its phenotype contrasts with those of previously reported mutants. First, only the apical part the endosperm is opaque, whereas the basal part exhibits no difference from the wild type (Figure 1), indicating that it does not belong to any of the four subgroups of opaque mutants listed above. Second, the *os1* mutant has a significantly smaller embryo than the wild type (Figure 1A), a phenotype that also has not been reported in previous opaque mutants. Finally, transmission electron micrography analysis indicated that the protein and starch granule bodies in the *os1*

mutant are sparser and smaller as compared to those of the wild type. Together, these results suggest that *os1* is a new opaque mutant, and that further investigation of this mutant could provide us more information to uncover the underlying molecular regulatory mechanisms in both embryo and endosperm development.

The opacity of *os1* endosperm might be related to loss of subaleurone cell layers in the crown

In the *os1* mutant, only the apical part of the endosperm shows starchy, whereas the basal part is indistinguishable from wild type (Figure 1B). SEM analysis indicated that the subaleurone cell layers of *os1* mutants were occupied by starchy cells, a point of partial similarity with the *nkd* mutant (Yi et al. 2015; Gontarek et al. 2016). In the *nkd* mutant, the single aleurone and subaleurone cell layers do not develop completely, resulting in starchy endosperm exposed to pericarp and then opaque endosperm (Gontarek et al. 2016). It has been reported that the ingredients of subaleurone cell layer have higher zein protein contents than the CSE (Kent 1966; Zheng and Wang 2014). Meanwhile, immunodetection showed that 27-kD γ-zein protein is enriched in the subaleurone cell layers adjacent to the single aleurone cell layer, but is barely detected in cells farther away from the subaleurone cell layers (Geetha et al. 1991).

Our analysis demonstrated that both the mRNA transcript and protein levels of 27-kD γ-zein were sharply decreased in both the upper and lower parts of the endosperm (Figure 2A). These results imply that the 27-kD γ-zein protein could also be decreased in the subaleurone cell layers of *os1* mutant endosperm. Together, our results indicate that there might be a direct or indirect relationship between opaque and loss of subaleurone in *os1* mutant, which needs to be further tested.

OS1 encodes a putative RWP-RK transcription factor with novel function

Our data demonstrate that OS1 encodes a putative RWP-RK domain-containing transcription factor with a regulatory function in maize seed development. The RWP-RK transcription factor family, named for its conserved DNA-binding domain, was first reported and named in legume species of *Lotus japonicus* (Schauser et al. 1999) upon isolation from a *nin* (*nodule inception*) mutant. The product of the *Nin* gene was reported to function as a regulator controlling root nodule initiation and development under low-nitrogen conditions (Schauser et al. 1999; Borisov et al. 2003).

Further bioinformatics analysis revealed that the RWP-RK family could be divided into two subclasses: the NLPs, with multiple functional domains and longer protein length (800–900 aa), and the RKDs, with only the RWP-RK DNA-binding domain and shorter protein length (~300 aa). *Arabidopsis* NLP-7, belonging to the NLP class, is thought to be involved in the nitrate sensing; loss-of-function mutants show several features of a nitrogen-starved phenotype in the leaf, as well as drought tolerance (Castaings et al. 2009). Meanwhile, five members of the RKD class, AtRKD1–5, are involved in early embryonic development, as well as gametophyte polarity and cell differentiation, in *Arabidopsis* (Jeong et al. 2011; Waki et al. 2011; Tedeschi et al. 2017).

All the known genes from the RWP-RK family are reported to encode proteins involved in root nodule development and early embryonic development in legume species or dicotyledonous plants, but not functionally analyzed in monocotyledonous plants, such as maize and rice. In our study, OS1, with only 331 amino acids, belongs to the RKD clade (Figure 6A), and we show that OS1 mainly functions in maize early endosperm development, which is very different from the pattern for the *Arabidopsis* RKD proteins.

These findings imply that OS1 plays a role in maize seed that is different from that of homologous RKD proteins in other species. However, from an evolutionary point of view, the function of OS1 in maize is partly conserved in comparison to those of RKD proteins in other species, in that it also affects nutritional pathways. Although we did not observe phenotypes consistent with nitrogen starvation in *os1* leaves at either seedling or adult stages, the opaque endosperm and smaller size of embryo might be considered as a type of nutrient-starved phenotype in kernel. However, what nutrients might be involved in the regulatory network mediated by OS1 remains to be discovered.

OS1 might be a master regulator in maize

So far, many genes corresponding to opaque and floury endosperm have been shown to encode enzymes involved in zein protein and starch synthesis (for example, Kim et al. 2004; Holding et al. 2007; Miclaus et al. 2011; Myers et al. 2011; Wang et al. 2011; Wang et al. 2012; Yao et al. 2016). But only a few regulators of endosperm development have been cloned and

functionally investigated: *O2*, *O11* and *floury 3* (Schmidt et al. 1990; Li et al. 2017; Feng et al. 2018).

In addition, all of these regulators show a kernel-specific expression pattern, and none of the corresponding mutants have detectable phenotypes besides opaque endosperm. However, we detected transcripts of *OS1* in almost all maize tissues, though its expression was highest in kernel. Furthermore, we show that *os1* mutants had other phenotypic traits, besides an opaque endosperm, such as smaller embryo size and increased anther number in tassel (Table S2). These results suggest that OS1 regulates multiple genes in different organs, which means that OS1 might be a master regulator in maize.

OS1 modulates expression of numerous zein genes

More than 60% of proteins, by weight, in the endosperm are zeins, also known as prolamins. These are mainly grouped into four classes according to their solubility in alcohol solutions: α (19- and 22-kD zeins), β (15-kD zein), γ (16-, 27- and 50-kD zeins) and δ (10- and 18-kD zeins) (Wallace et al. 1990). It has been reported that 22-kD α-zein is directly bound by the transcription factor O2 (Lending and Larkins 1989; Schmidt et al. 1992; Muth et al. 1996). Moreover, other zeins, such as the 10-, 15- and 19-kD zeins, show decreased accumulation of mRNA transcripts (Cord et al. 1995; Hunter et al. 2002; Wu et al. 2010).

Recent chromatin immunoprecipitation and sequencing (ChIP-Seq) and RNA-Seq investigations of the *o2* mutant demonstrated that it directly or indirectly affects almost all of the zein genes at the transcriptional level, as well as transcription factors (Li et al. 2015; Zhan et al. 2018). More interestingly, the transcription factors activated by O2 could also co-activate other O2-network genes together with O2 (Zhan et al. 2018). The other important transcription factors involved in the regulation of zein proteins in maize endosperm are prolamin-box binding factor (PBF) and Opaque2 heterodimerizing protein (OHP). Members of this family could act as a dimer to co-regulate expression of zein genes (Zhang et al. 2015; Yang et al. 2016). The ZmMADS47, belonging to MADS-domain transcription factor family, can also coactivate a number of zein genes through interaction with O2 (Qiao et al. 2016).

The central regulator O11, belonging to the basic helix-loop-helix (bHLH) transcription factor family, was demonstrated to influence development and nutrient metabolism of endosperm by directly binding transcription factors, such as *NKD2* and *ZmDof3*, as well as *O2* and *PBF*. These results suggest that the storage protein regulatory pathway is mainly regulated by upstream and downstream effects of O2, as well as its coactivators.

Our data indicated that many zein genes and some starch synthetic genes were significantly downregulated in the *os1* mutant. The phenotype is consistent with the mutants having decreased accumulation of zein proteins. Furthermore, we did not observe significant changes in expression level of *O2* in our RNA-Seq data. This implies that OS1 might be part of a separate pathway or co-work with O2 regulating storage proteins and starch in maize endosperm. Taken together, these data show that OS1 represents a previously unknown pathway, separate from the O2 network or working with O2, for regulating development and nutrient metabolism in maize endosperm. However, more data are needed to verify what relationship there may be between OS1 and O2.

OS1 mediates resource allocation from endosperm to embryo

Photosynthesis products are transported from leaves to sink organs such as seeds. The BETL, which forms adjacent to the pedicel tissue of the maternal plant, is one of the earliest endosperm cell types to differentiate and plays a key role in facilitating maternal solute uptake into starchy cells and embryo cells. Thus, mutants affecting BETL cells would be expected to result in developmental defects or unsuccessful grain filling, ultimately leading to smaller seeds or defective kernels.

Loss of function of *Meg1* directly affects the differentiation of BETL cells, resulting in smaller seed (Costa et al. 2012). The BETL-specifically expressed gene Mn1 encodes an invertase involved in the degradation of sucrose into fructose and glucose, and mutation of *Mn1* leads to a smaller seed with a normal embryo (Miller and Chourey 1992). Thus, all of these mutants affecting the differentiation of BETL cells result in smaller kernel size.

In our study, the BETL cells of *os1* mutants differentiated completely normally, as did the ESR cells (Figure S4). Meanwhile, although the *os1* mutant has a smaller embryo, its seed size and seed weight are almost the same as in wild type (Figure 1). These results

suggest that *OS1* is not involved in the differentiation of the BETL, BIZ, CZ or ESR cell types, but only in the nutrient allocation between endosperm and embryo within the seed.

Interestingly, our RNA-Seq data showed that many marker genes specifically expressed in cell types involved in nutrient transport and allocation, such as BETL, BIZ and CZ cells, were significantly downregulated in *os1* endosperm at 6 DAP. Moreover, the expression of *OS1* was also enriched in BETL, BIZ and CZ cell types of the endosperm (Figure 8E), which also fits with the endosperm's functional role as a nutrient allocator. However, many of the differentially expressed genes were not functionally characterized. Therefore, identifying factors definitely involved in nutrient transport from endosperm to embryo will be a key step in further elucidating the function of OS1.

Collectively, our findings demonstrate that maize *OS1* is a previously unidentified transcription factor controlling seed development. Functional analysis revealed that this protein has roles in endosperm and embryo development, as well as effects in other non-seed tissues, a pattern that is unique to this protein as compared to its orthologs in legumes and other dicotyledonous species. Therefore, further study of the functions of OS1 and its regulatory networks will provide new clues for elucidating the process of nutrient allocation within seed, as well as new opportunities for genetically improving seed quality in maize.

MATERIALS AND METHODS

Plant materials

The *os1* mutant was isolated from a natural breeding population (Song and Lu 1993). The mutant was crossed with wild-type (*Zea mays*) Mo17 to obtain F1 progeny, and then the F1 progeny were backcrossed with os1 and self-pollinated to obtain the two genetic mapping populations BC1F1 and F2, respectively. These materials were planted at the Shangzhuang research station of the China Agricultural University in the Haidian district of Beijing.

After harvest, kernels were detached from different ears and grouped based on seed phenotype. The kernels were then planted in seed plots (5×10 grids per plot) and were grown in growth chambers at 32/23°C (day/night) for germination; humidity was controlled at approximately 50%. Seven days later, the leaves of the seedling were dissected for DNA extraction.

Genetic mapping of *OS1*

A large BC1F1 population, containing more than 10,000 plants, was used for genetic mapping of the *OS1* gene. First, 93 plants with the mutant phenotype were selected for preliminary mapping, through which the *os1* locus was localized to the bin 2.03 region of chromosome 2, between the two simple sequence repeat (SSR) markers umc1845 and umc2193 (the sequences of primers were downloaded from http://www.maizegdb.org/). For fine mapping of *OS1*, 3,252 BC1F1 individuals were screened using the SSR markers P1-P10 that we developed. The PCR products were digested with the restriction enzyme *Msp*I. Finally, the os1 locus was located within a 250-kb region flanked by the P7 and P9 markers.

Scanning electron microscopy (SEM) and transmission electron microscopy (TEM)

Mature mutant and wild-type seeds from the same ear were split using two forceps and then observed by SEM (Hitachi S-4700). For TEM observation, 18-DAP immature mutant and wild-type seeds were collected, and fixed by using of paraformaldehyde and post-fixed in osmium tetroxide, at room temperature, embedded in epoxide resin and section (60-nm thickness). The samples were observed by TEM (Hitachi H7600).

Double haploid system for embryo rescue and measurements of kernel related traits

The mutant was used as the female in this double haploid system and different kernel type classification, was as previously described (Tian et al. 2018). In brief, the *os1*/*os1* homozygous mutant was used as the female in this cross, and the *os1*/*os1* pollen was mixed with CAU05 pollen with equal volume. The length and area of the kernel, embryo was measured by photographing, the images were edited for data collection (kernel length and width, embryo length and width, as well as embryo area) by using of software Photoshop CS6.

Measurements of amino acids, crude proteins, zeins, carbohydrate, and lipids

Forty mature seeds from one ear, a mixture of *os1* mutant and wild-type phenotypes, were collected and soaked in water for 12 h. Then, the embryo, endosperm

and pericarp of the *os1* mutant were separated. For measurements of zeins and non-zein proteins from upper and lower endosperm, the endosperm of mutant and wild-type seeds was separated based on the line opacity (Figure 1B). The separated embryo, full endosperm, upper endosperm and lower endosperm were ground into powder using a manual grinder for subsequent measurements.

For crude protein and amino acid measurements, the total protein (crude protein) was extracted from kernel, embryo and endosperm, hydrolyzed into amino acids and then used for subsequent analysis by liquid phase chromatography. Measurement of carbohydrate in endosperm was as previously described (Wang et al. 2015). Measurement of lipids in the kernel was performed, as previously described (Li et al. 2013). For each assay, three biological replicates were performed, as well as three parallel repeats for each biological replicate.

The zein proteins and non-zein proteins were extracted from whole endosperm, upper endosperm and lower endosperm, as previously described (Liu et al. 2016). SDS-PAGE analysis was performed to measure the accumulation patterns of zein and non-zein proteins in the *os1* mutant and wild type.

Light microscopy of cytological sections

Analysis of cytological section was performed, as previously described (Li et al. 2018). In brief, immature *os1* mutant and wild-type kernels were collected from the same segregating ears of 6 DAP. Then, the cut central kernel containing the embryo and partial endosperm were fixed in FAA overnight, following dehydration, clearing and wax infiltrating. Finally, the samples were sectioned at 6 mm with a Leica RM2235 slicer.

Statistical analysis

The Student's *t*-test was used to detect significant differences ($P < 0.01$ or 0.05) between mutant and wild type. Data from biological replicates were analyzed in each measurement, and were presented in the figures as the mean of replicates $\pm$ *SD*.

Construction of vector and maize transformation

For complementation of the *os1* mutant, a fragment of genomic DNA containing 7.0 kb of gene body containing promoter and terminator of *OS1* gene from wild type, was cloned into a binary vector pCAMBIA3301 by using the *HindIII* and *BamHI* sites. Transformation of the HiII maize strain with *Agrobacterium tumefaciens* strain EHA105 harboring the complementation vector was performed, as previously described (Vega et al. 2008). In brief, ears of HiIIA and HiIIB were harvested from field 10–13 d after pollination (DAP) reciprocally and sterilized, and their embryos were then dissected. Immature embryos dissected from the sterilized ears were incubated for 10 min with *Agrobacterium tumefaciens* harboring the complementation vector and cultured on the co-culture medium for 3 d. Then, the embryos were transferred onto the resting medium, and selection medium. After 3–4 weeks of selection, calli with bialaphos resistance were used for regeneration, and genotyping.

Screening on the mu1-based mutant library and allelism test

The mutant library was constructed by crossing elite inbred Zong31 and a mutator line; the F_1 seedlings were planted in the field and 20,000 self-pollinated ears were ultimately harvested. We screened the self-pollinated ears for the phenotype of opaque endosperm and smaller embryo size. The accession L17627 had the same mutant phenotype as *os1* and was named *os1-mu1*. Sequence analysis of *os1-mu1* revealed that there is a 1.3-kb mutator insertion in the second exon of the *OS1* candidate gene. To confirm the allelic relationship between *os1* and *os1-mu1*, we reciprocally crossed homozygous *os1* plants with homozygous *os1-mu1* plants.

Subcellular localization and confocal microscopy

To determine the subcellular localization of the OS1 protein, cDNA containing the open reading frame of *OS1* was amplified by RT-PCR (File S1), and then the PCR product was digested with the restriction enzymes *BamH1* and *Xba1* and cloned into the *GFP* reporter-gene fusion vector Pmon30049. The constructs, including *GFP::OS1*, as well as the empty vector Pmon30049, were transformed into onion epidermal cells and fluorescence was imaged under a NIKON D-Eclipse C1, TE2000-E confocal microscope.

Reverse transcriptase quantitative real-time PCR

Total RNA was extracted from different tissues of field-grown B73 inbred lines at the 15-leaf stage, namely

roots, stem, leaves, 12-cm tassels, 3-cm ears and anthers. First-strand cDNAs were synthesized from total RNA using SuperScript II reverse transcriptase (Invitrogen, USA). Real-time RT-qPCR was performed using a SYBR® Premix Ex Taq™ (Perfect Real Time: TaKaRa) on an ABI7500 machine (USA: ABI). Each 30-μL PCR reaction contained 15 μL of 2× SYBR Green Premix, 10 μL of cDNA, 0.6 μL forward and 0.6 uL reverse primers (10 uM) and 0.6 μL of ROX Reference Dye II. PCR was performed starting with a holding stage at 95°C for 2 min, which was followed by 40 cycles of denaturation at 95°C for 15 s, annealing at 60°C for 34 s and extension at 72°C for 15 s. All the quantitative assays were performed three times on each cDNA sample. The primers used for RT-qPCR are listed in File S1.

Bombardment delivery and GFP transient expression

Gold particle preparation and bombardment were performed, as previously described (Sanford 1993). The onion skins were divided into 30 mm × 30 mm pieces and were placed on base medium containing 4.3 g MS salts (Murashige and Skoog 1962) and 0.8% agar powder, with the pH adjusted to pH 7.0. 300 ng of the plasmid carrying the GFP and fusion vectors was used for each bombardment. After bombardment, the plates were transferred to a growth chamber, in darkness, at 28°C for 24 h, and then the epithelial tissues were transferred onto the slides and the fluorescent images were observed under the confocal microscope.

Library construction and RNA-Seq analysis

Two biological replicates were used for RNA isolation, library construction and later sequencing. Total RNA was extracted from 6-DAP and 14-DAP endosperm of wild-type and mutant seeds, as well as other tissues, for RT-qPCR by using of Trizol reagent (Invitrogen). The RNA-Seq libraries were constructed and then subjected to Illumina sequencing in Hiseq2000, as previously described (Song et al. 2016). After sequencing, raw reads were aligned to the B73 reference genome (v3) using Tophat 2.0.6 (Trapnell et al. 2009) with default settings for all parameters. The differentially expressed genes were defined by the thresholds of a *P*-value < 0.05 (Student's *t*-test) and a fold change > 2.0. The relative expression levels of DEGs in the RNA-Seq analysis were denoted in fragments per kilobase of exon per million fragments mapped. Two biological replicate samples were performed for the *os1* mutant and the wild type, and three technical validations were performed for each biological replication. The GO enrichment analysis of downregulated DEGs was performed using MapMan annotation (Thimm et al. 2004).

***In situ* hybridization**

Maize seeds were dissected from 4-DAP, 6-DAP, 8-DAP and 10-DAP field-grown plants. Tissue sections and *in situ* hybridization were conducted, as previously described (Zhang et al. 2015). Digoxigenin-labeled probes were prepared using DIG RNA Labeling Kit (SP6/T7) (Roche). At least 10 replicate samples were analyzed for each time point. The probe of *OS1* was listed in File S3.

ACKNOWLEDGEMENTS

We thank Xiaomin Lu and Yongbin Dong for screening the second allele of *os1-mu1* in the field and Yuanyuan Xu for performing the semi-quantitative RT-PCR. We also thank the Xiaohong Yang lab and Yongrui Wu lab for helping to measure seed nutrients and *in situ* hybridization experiments, as well as Baojian Chen, Shaojiang Chen lab, for providing CAU05 and oil measurement. This work was supported by the National Natural Science Foundation program of China (31671698), and National Key Research & Development Program (2016YFD0100404, 2017YFD0101104).

AUTHOR CONTRIBUTIONS

J.L. and W.S. designed the research, performed the data analysis, and wrote the manuscript; W.S., J.Z., H.Z., J.L., Y.L., X.Z., L.H., and J.L. performed the data collection and analysis; all authors discussed the data, and read and approved the contents of this manuscript.

REFERENCES

Becraft PW (2001) Cell fate specification in the cereal endosperm. **Semin Cell Dev Biol** 12: 387–394

Becraft PW, Gutierrez-Marcos J (2012) Endosperm development: Dynamic processes and cellular innovations

underlying sibling altruism. **Wiley Interdiscip Rev Dev Biol** 1: 579–593

Borisov AY, Madsen LH, Tsyganov VE, Umehara Y, Voroshilova VA, Batagov AO, Sandal N, Mortensen A, Schauser L, Ellis N, Tikhonovich IA, Stougaard J (2003) The *Sym35* gene required for root nodule development in pea is an ortholog of *Nin* from *Lotus japonicus*. **Plant Physiol** 131: 1009–1017

Castaings L, Camargo A, Pocholle D, Gaudon V, Texier Y, Boutet-Mercey S, Taconnat L, Renou JP, Daniel-Vedele F, Fernandez E, Meyer C, Krapp A (2009) The nodule inception-like protein 7 modulates nitrate sensing and metabolism in *Arabidopsis*. **Plant J** 57: 426–435

Chardin C, Girin T, Roudier F, Meyer C, Krapp A (2014) The plant RWP-RK transcription factors: Key regulators of nitrogen responses and of gametophyte development. **J Exp Bot** 65: 5577–5587

Chen J, Zeng B, Zhang M, Xie S, Wang G, Hauck A, Lai J (2014) Dynamic transcriptome landscape of maize embryo and endosperm development. **Plant Physiol** 166: 252–264

Coleman CE, Clore AM, Ranch JP, Higgins R, Lopes MA, Larkins BA (1997) Expression of a mutant alpha-zein creates the floury2 phenotype in transgenic maize. **Proc Natl Acad Sci USA** 94: 7094–7097

Cord NG, Yunes JA, Da SM, Vettore AL, Arruda P, Leite A (1995) The involvement of Opaque 2 on beta-prolamin gene regulation in maize and *Coix* suggests a more general role for this transcriptional activator. **Plant Mol Biol** 27: 1015–1029

Costa LM, Yuan J, Rouster J, Paul W, Dickinson H, Gutierrez-Marcos JF (2012) Maternal control of nutrient allocation in plant seeds by genomic imprinting. **Curr Biol** 22: 160–165

Feng F, Qi W, Lv Y, Yan S, Xu L, Yang W, Yuan Y, Chen Y, Zhao H, Song R (2018) Opaque11 is a central hub of the regulatory network for maize endosperm development and nutrient metabolism. **Plant Cell** 30: 375–396

Geetha KB, Lending CR, Lopes MA, Wallace JC, Larkins BA (1991) Opaque-2 modifiers increase gamma-zein synthesis and alter its spatial distribution in maize endosperm. **Plant Cell** 3: 1207–1219

Gontarek BC, Neelakandan AK, Wu H, Becraft PW (2016) NKD Transcription factors are central regulators of maize endosperm development. **Plant Cell** 28: 2916–2936

Holding DR, Otegui MS, Li B, Meeley RB, Dam T, Hunter BG, Jung R, Larkins BA (2007) The maize *floury1* gene encodes a novel endoplasmic reticulum protein involved in zein protein body formation. **Plant Cell** 19: 2569–2582

Hong SK, Kitano H, Satoh H, Nagato Y (1996) How is embryo size genetically regulated in rice? **Development** 122: 2051–2058

Hunter BG, Beatty MK, Singletary GW, Hamaker BR, Dilkes BP, Larkins BA, Jung R (2002) Maize opaque endosperm mutations create extensive changes in patterns of gene expression. **Plant Cell** 14: 2591–2612

Jeong S, Palmer TM, Lukowitz W (2011) The RWP-RK factor *GROUNDED* promotes embryonic polarity by facilitating YODA MAP kinase signaling. **Curr Biol** 21: 1268–1276

Kent NL (1966) Subaleurone endosperm cells of high protein content. **Cereal Chem** 43: 585–601

Kim CS, Hunter BG, Kraft J, Boston RS, Yans S, Jung R, Larkins BA (2004) A defective signal peptide in a 19-kD-zein protein causes the unfolded protein response and an opaque endosperm phenotype in the maize *de*-B30* mutant. **Plant Physiol** 134: 380–387

Kim CS, Gibbon BC, Gillikin JW, Larkins BA, Boston RS, Jung R (2006) The maize *Mucronate* mutation is a deletion in the 16-kDa gamma-zein gene that induces the unfolded protein response. **Plant J** 48: 440–451

Lending CR, Larkins BA (1989) Changes in the zein composition of protein bodies during maize endosperm development. **Plant Cell** 1: 1011–1023

Leroux BM, Goodyke AJ, Schumacher KI, Abbott CP, Clore AM, Yadegari R, Larkins BA, Dannenhoffer JM (2014) Maize early endosperm growth and development: From fertilization through cell type differentiation. **Am J Bot** 101: 1259–1274

Li C, Qiao Z, Qi W, Wang Q, Yuan Y, Yang X, Tang Y, Mei B, Lv Y, Zhao H, Xiao H, Song R (2015) Genome-wide characterization of cis-acting DNA targets reveals the transcriptional regulatory framework of opaque2 in maize. **Plant Cell** 27: 532–545

Li G, Wang D, Yang R, Logan K, Chen H, Zhang S, Skaggs MI, Lloyd A, Burnett WJ, Laurie JD, Hunter BG, Dannenhoffer JM, Larkins BA, Drews GN, Wang X, Yadegari R (2014) Temporal patterns of gene expression in developing maize endosperm identified through transcriptome sequencing. **Proc Natl Acad Sci USA** 111: 7582–7587

Li H, Peng Z, Yang X, Wang W, Fu J, Wang J, Han Y, Chai Y, Guo T, Yang N, Liu J, Warburton ML, Cheng Y, Hao X, Zhang P, Zhao J, Liu Y, Wang G, Li J, Yan J (2013) Genome-wide association study dissects the genetic architecture of oil biosynthesis in maize kernels. **Nat Genet** 45: 43–50

Li Q, Wang J, Ye J, Zheng X, Xiang X, Li C, Fu M, Wang Q, Zhang Z, Wu Y (2017) The maize imprinted gene *floury3* encodes a PLATZ protein required for tRNA and 5S rRNA transcription through interaction with RNA polymerase III. **Plant Cell** 29: 2661–2675

Li X, Gu W, Sun S, Chen Z, Chen J, Song W, Zhao H, Lai J (2018) Defective Kernel 39 encodes a PPR protein required for seed development in maize. **J Integr Plant Biol** 60: 45–64

Liu H, Shi J, Sun C, Gong H, Fan X, Qiu F, Huang X, Feng Q, Zheng X, Yuan N, Li C, Zhang Z, Deng Y, Wang J, Pan G, Han B, Lai J, Wu Y (2016) Gene duplication confers enhanced expression of 27-kDa gamma-zein for endosperm modification in quality protein maize. **Proc Natl Acad Sci USA** 113: 4964–4969

Lopes MA, Larkins BA (1993) Endosperm origin, development, function. **Plant Cell** 5: 1383–1399

Miclaus M, Wu Y, Xu JH, Dooner HK, Messing J (2011) The maize high-lysine mutant *opaque7* is defective in an acyl-CoA synthetase-like protein. **Genetics** 189: 1271–1280

Miller ME, Chourey PS (1992) The maize invertase-deficient miniature-1 seed mutation is associated with aberrant pedicel and endosperm development. **Plant Cell** 4: 297–305

Muth JR, Muller M, Lohmer S, Salamini F, Thompson RD (1996) The role of multiple binding sites in the activation of zein gene expression by Opaque-2. **Mol Gen Genet** 252: 723–732

Myers AM, James MG, Lin Q, Yi G, Stinard PS, Hennen-Bierwagen TA, Becraft PW (2011) Maize opaque5 encodes monogalactosyldiacylglycerol synthase and specifically affects galactolipids necessary for amyloplast and chloroplast function. **Plant Cell** 23: 2331–2347

Neuffer MG, Sheridan WF (1980) Defective kernel mutants of maize. I. genetic and lethality studies. **Genetics** 95: 929–944

Olsen OA (2001) Endosperm development: Cellularization and cell fate specification. **Annu Rev Plant Physiol Plant Mol Biol** 52: 233–267

Qiao Z, Qi W, Wang Q, Feng Y, Yang Q, Zhang N, Wang S, Tang Y, Song R (2016) ZmMADS47 regulates zein gene transcription through interaction with opaque2. **PLoS Genet** 12: e1005991

SabelLi PA, Larkins BA (2009) The contribution of cell cycle regulation to endosperm development. **Sex Plant Reprod** 22: 207–219

Schauser L, Roussis A, Stiller J, Stougaard J (1999) A plant regulator controlling development of symbiotic root nodules. **Nature** 402: 191–195

Schmidt RJ, Burr FA, Burr B (1987) Transposon tagging and molecular analysis of the maize regulatory locus opaque-2. **Science** 238: 960–963

Schmidt RJ, Burr FA, Aukerman MJ, Burr B (1990) Maize regulatory gene opaque-2 encodes a protein with a "leucine-zipper" motif that binds to zein DNA. **Proc Natl Acad Sci USA** 87: 46–50

Schmidt RJ, Ketudat M, Aukerman MJ, Hoschek G (1992) Opaque-2 is a transcriptional activator that recognizes a specific target site in 22-kD zein genes. **Plant Cell** 4: 689–700

Song T, Lu X (1993) The chromosomal location and inheritance of a new corn kernel mutant gene (os) with pleiotropic effects. **Acta Genet Sin** 20: 432–438

Song W, Zhao H, Zhang X, Lei L, Lai J (2016) Genome-wide identification of VQ motif-containing proteins and their expression profiles under abiotic stresses in maize. **Front Plant Sci** 6: 1177

Tedeschi F, Rizzo P, Rutten T, Altschmied L, Baumlein H (2017) RWP-RK domain-containing transcription factors control cell differentiation during female gametophyte development in *Arabidopsis*. **New Phytol** 213: 1909–1924

Thimm O, Blasing O, Gibon Y, Nagel A, Meyer S, Kruger P, Selbig J, Muller LA, Rhee SY, Stitt M (2004) MAPMAN: A user-driven tool to display genomics data sets onto diagrams of metabolic pathways and other biological processes. **Plant J** 37: 914–939

Thompson RD, Hueros G, Becker H, Maitz M (2001) Development and functions of seed transfer cells. **Plant Sci** 160: 775–783

Tian X, Qin Y, Chen B, Liu C, Wang L, Li X, Dong X, Liu L, Chen S (2018) Hetero-fertilization along with failed egg-sperm cell fusion supports single fertilization involved in *in vivo* haploid induction in maize. **J Exp Bot** 69: 4689–4701

Trapnell C, Pachter L, Salzberg SL (2009). TopHat: discovering splice junctions with RNA-Seq. **Bioinformatics** 25: 1105–1111

Vega JM, Yu W, Kennon AR, Chen X, Zhang ZJ (2008) Improvement of *Agrobacterium*-mediated transformation in Hi-II maize (*Zea mays*) using standard binary vectors. **Plant Cell Rep** 27: 297–305

Waki T, Hiki T, Watanabe R, Hashimoto T, Nakajima K (2011) The *Arabidopsis* RWP-RK protein RKD4 triggers gene expression and pattern formation in early embryogenesis. **Curr Biol** 21: 1277–1281

Wallace JC, Lopes MA, Paiva E, Larkins BA (1990) New methods for extraction and quantitation of zeins reveal a high content of gamma-zein in modified opaque-2 maize. **Plant Physiol** 92: 191–196

Wang G, Qi W, Wu Q, Yao D, Zhang J, Zhu J, Wang G, Wang G, Tang Y, Song R (2014) Identification and characterization of maize floury4 as a novel semidominant opaque mutant that disrupts protein body assembly. **Plant Physiol** 165: 582–594

Wang G, Wang F, Wang G, Wang F, Zhang X, Zhong M, Zhang J, Lin D, Tang Y, Xu Z, Song R (2012) Opaque1 encodes a myosin XI motor protein that is required for endoplasmic reticulum motility and protein body formation in maize endosperm. **Plant Cell** 24: 3447–3462

Wang G, Sun X, Wang G, Wang F, Gao Q, Sun X, Tang Y, Chang C, Lai J, Zhu L, Xu Z, Song R (2011) Opaque7 encodes an acyl-activating enzyme-like protein that affects storage protein synthesis in maize endosperm. **Genetics** 189: 1281–1295

Wang T, Wang M, Hu S, Xiao Y, Tong H, Pan Q, Xue J, Yan J, Li J, Yang X (2015) Genetic basis of maize kernel starch content revealed by high-density single nucleotide polymorphism markers in a recombinant inbred line population. **BMC Plant Biol** 15: 288

Wu Y, Messing J (2010) Rescue of a dominant mutant with RNA interference. **Genetics** 186: 1493–1496

Wu Y, Holding DR, Messing J (2010) Gamma-zeins are essential for endosperm modification in quality protein maize. **Proc Natl Acad Sci USA** 107: 12810–12815

Yang J, Ji C, Wu Y (2016) Divergent transactivation of maize storage protein zein genes by the transcription factors opaque2 and OHPs. **Genetics** 204: 581–591

Yao D, Qi W, Li X, Yang Q, Yan S, Ling H, Wang G, Wang G, Song R (2016) Maize opaque10 encodes a cereal-specific protein that is essential for the proper distribution of zeins in endosperm protein bodies. **PLoS Genet** 12: e1006270

Yi G, Neelakandan AK, Gontarek BC, Vollbrecht E, Becraft PW (2015) The naked endosperm genes encode duplicate *INDETERMINATE* domain transcription factors required for maize endosperm cell patterning and differentiation. **Plant Physiol** 167: 443–456

Zhan J, Thakare D, Ma C, Lloyd A, Nixon NM, Arakaki AM, Burnett WJ, Logan KO, Wang D, Wang X, Drews GN, Yadegari R (2015) RNA sequencing of laser-capture microdissected compartments of the maize kernel

identifies regulatory modules associated with endosperm cell differentiation. **Plant Cell** 27: 513–531

Zhan J, Li G, Ryu CH, Ma C, Zhang S, Lloyd A, Hunter BG, Larkins BA, Drews GN, Wang X, Yadegari R (2018) Opaque-2 regulates a complex gene network associated with cell differentiation and storage functions of maize endosperm. **Plant Cell** 30: 2425–2446

Zhang S, Zhan J, Yadegari R (2018) Maize opaque mutants are no longer so opaque. **Plant Reprod** 31: 319–326

Zhang Z, Yang J, Wu Y (2015) Transcriptional regulation of zein gene expression in maize through the additive and synergistic action of opaque2, prolamine-box binding factor, O2 heterodimerizing proteins. **Plant Cell** 27: 1162–1172

Zheng Y, Wang Z (2014) Protein accumulation in aleurone cells, sub-aleurone cells and the center starch endosperm of cereals. **Plant Cell Rep** 33: 1607–1615

SUPPORTING INFORMATION

Additional Supporting Information may be found online in the supporting information tab for this article: http://onlinelibrary.wiley.com/doi/10.1111/jipb.12755/suppinfo

Figure S1. Measurements of ear-related traits in the mutant and wild type maize plants

(A) Ear length. **(B)** Ear diameter. **(C)** Ear row number.

Figure S2. Results of allelism test for *os1* and *os1-mu1* lines

(A, B) Genome sequencing of candidate genes in *os1* (**A**) and *os1-mu1* (**B**) materials showed that both mutants contain transposon insertions in the second exon of the candidate gene. (**C**) Hybrid seeds of the two mutants (*os1* × *os1-mu1*), as well as those of *os1* and *os1-mu1*, showed the same phenotype.

Figure S3. Schematic diagrams of various constructs used for transactivation activity assays

(A) The numbers in the different constructs represent the position of amino acids of OS1 protein. **(B)** The six constructs that were transformed into yeast and transferred to media with different nutrient deficiencies. DNA-BD, DNA-binding domain; RING5-BD, RING5 DNA-binding domain; RING1-AD, RING1 active domain.

Figure S4. Longitudinal sections of 8-DAP kernels from wild-type and mutant plants

(A) Wild-type kernel including developing embryo and endosperm. **(B)** Mutant-type kernel including developing embryo and endosperm. **(C)** Enlarged parts of wild-type kernel from yellow frame in **(A)**. **(D)** Enlarged parts of mutant-type kernel from yellow frame in **(B)**. em (embryo), en (endosperm), BETL (basal endosperm transfer layer), PC, (placento-chalazal region).

Table S1. Complementation analysis of the *os1* mutant

Table S2. Phenotypic analysis of the *os1* mutant inflorescence

File S1. Molecular markers used during fine mapping

File S2. The amino sequences of RWP-RK genes from different species

File S3. *OS1* probe for *in situ* hybridization

File S4. DEGs at 6 and 14 DAP

File S5. Gene accessions for the heat map

Scan using WeChat with your smartphone to view JIPB online

Scan with iPhone or iPad to view JIPB online